AIMS Energy, 10(2): 340–355.
DOI: 10.3934/energy.2022018
Received: 03 April 2022
Revised: 20 April 2022
Accepted: 21 April 2022
Published: 16 May 2022

http://www.aimspress.com/journal/energy

Research article

Investigation of the effect of the injection pressure on the direct-ignition diesel engine performance

Saad S. Alrwashdeh[1,2,*]

[1] Mechanical Engineering Department, Faculty of Engineering, Mutah University, P.O Box 7, Al-Karak 61710 Jordan
[2] Materials Science and Energy Lab, MSEL. Mutah University, P.O Box 7, Al-Karak 61710 Jordan

* **Correspondence:** Email: saad.alrwashdeh@mutah.edu.jo; Tel: +962796430481.

Abstract: Internal combustion engines (ICE) play a major role in converting the energy with its different types in order to benefit from it for various applications such as transportation, energy generation, and many others applications. Internal combustion engines use two main types of operation cycles, namely the Otto and Diesel cycles. Many development processes are carried out to improve the efficiency of the ICE nowadays such as working on the design of the combustion engine and the material selections and others. One of the main parameters which play an important role in improving the diesel engine is the fuel pressure. By increasing the fuel pressure injected into the engine, the efficiency, in consequence, will increase. This work investigates the injection pressure of the fuel (Diesel) and studies the effect of these changes on engine efficiency. It was found that the increase in injection pressure significantly affected the improvement in engine performance. Such improved engine subsystems will have a great impact on the energy extracted and used for various engineering applications.

Keywords: internal combustion engines; engine efficiency; injection pressure; diesel engines; operating cycles

1. Introduction

Combustion engines are major energy converters. As they convert the chemical energy stored in different types of fuel into thermal energy after direct and indirect combustion, then into mechanical energy. Converted energy is used in various engineering applications like transport with its different types and other different applications [1–3]. Combustion engines can be classified into different classifications based on a set of bases upon which it depends, the most important of which is the combustion site. Combustion engines can be categorized according to the location of combustion in external and internal combustion engines [4–6]. The engine that burns the fuel out and then transfers the energy to it is called the external combustion engine. The engine that burns the fuel inside it and benefits directly from it is called the internal combustion engine [7–11].

Combustion engines are regarded as the foundation of processes to benefit from different energy applications of different types, both traditional and renewable. The engine input comes from different sources, but by using the engine the end product is achieved which is mechanical energy [12,13].

Internal combustion engines are considered the most popular nowadays because of their efficiency and ease of handling. These engines rely on various heat cycles, the best known of which are the Otto and Diesel cycles [14–16]. The difference in thermal cycles in the internal combustion engines is fundamental and depends on the type of fuel types used [17–21]. The primary fuel of the Otto cycle is gasoline and the diesel cycle is diesel fuel [22]. The difference in the type of fuel used is the main reason for the difference in the installation and design of the engine. It's because each kind of fuel has its own nature [23–27].

In the development processes of combustion engines, including internal combustion engines. Many researchers around the world have done research on this topic such as, Jafari [28] who concerns about developing an active thermo atmospheric combustion. Negoro et al. [29] study the development of Toyota cars by improving the control of the combustion to be an auto-ignition that ensures more stability inside the engines. Doppalapudi et al. [30] studied the effect of the thermal stresses on parts of the engines such as the piston, connecting rods, and the pin. Where they found that the pressure on the engine pistons of the engine plays an important role in transforming the engine load from the combustion chamber. Which is located inside the cylinder connected to the crankshaft of the engine through the connecting rod.

Depending on the type of fuel used, this has an impact on the design of the engine [1,31–33]. The gasoline engine uses the spark plug to finish the combustion of the used fuel and thus complete the engine cycles and benefit from it [34–38]. In the case of the diesel engine, it adopts the self-combustion system. Results from increased the fuel pressure after pumping it through a sprayer until it reaches a point where the direct combustion condition is met. Thus completing the cycle and taking advantage of it [39–42].

Diesel engines are a major type of engines used nowadays. Due to their great advantages in various engineering areas, they provide high efficiency, and an ideal capability to complete various engineering operations. One of the most important of these applications is the transportation of various types, either by land or marine [43–45]. Diesel engines are also used in energy generation, as conventional electric generators use diesel engines due to their durability [46,47]. Diesel engines are considered to be energy efficient. As their fuel consumption depends on the amount of load it performs which is considered less fuel consumption compared with other types of engines [48–52]. Diesel engines are also considered to be one of the safest engines, due to the difficulty of igniting diesel

compared to other types of fuel that are used in engines. One of the advantages of using diesel engines is that they produce more torque than other engines at lower rpm levels [53,54].

Since diesel engines were invented until now. The science of engines in general and diesel engines, in particular, has been extensively developed and improved to increase the efficiency of these engines. The developments that the engines have encountered are: the development of the shapes and designs of the combustion chambers, the surfaces of the engine cylinders, and the materials from which the engine is made with its different parts [55–60]. Beside the developments that occurred in the engine itself. It was accompanied by a series of improvements and developments in the auxiliary systems of the engine. Which led to the development of the engine's efficiency. These systems include cooling, lubricating, fueling, etc. [61–63].

Diesel engines operate within high altitude zone, where the air pressure and density gradually decrease with increasing in altitude. As a result, diesel engines are injected with less air during the intake stroke, causing a decrease in the efficiency of the diesel engine [64]. The turbocharger came as a solution to this issue, as the efficiency of using the turbocharger has been studied by many researchers around the world. Using a turbocharger is not easy because it requires much equipment and most medium and small diesel engines are not equipped with such technology [65–68]. A proposed solution to these problems is the use of different types of fuels in diesel engines, such as oils of various types and other types of fuel which may operate under these operating conditions. [69–73].

In this work, the effect of changing the pressure of the diesel injected into the engine has been investigated. To investigate the effect of pressure modification on engine performance. It was found that by increasing the diesel fuel injection pressure significantly improved engine performance. Where the used pressure in the first case was less than 500 bar, the second case a pressure between 500 and 800 bar, the third case pressure within 800 to 1000, and the last case a pressure higher than 1000 bar.

2. Theoretical background

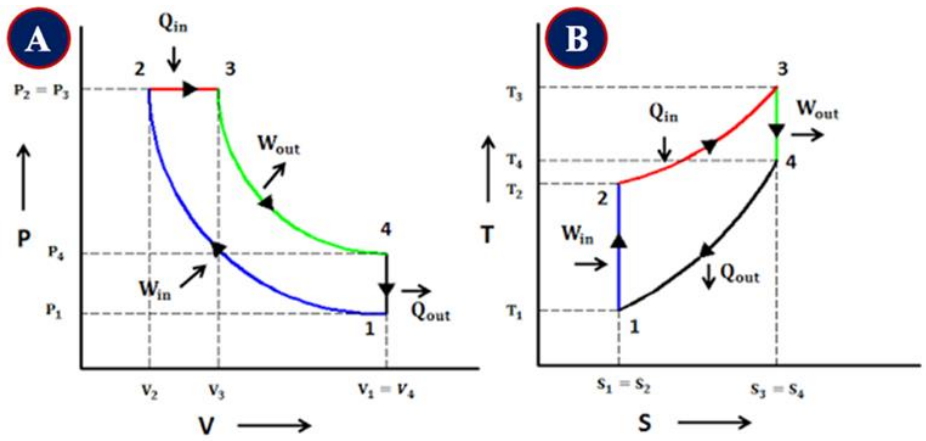

Figure 1. The P-V, and T-S diagrams of diesel cycle (A,B) respectively.

Rudolf diesel in 1892 introduced the diesel cycle as an internal combustion engine compression cycle. Figure 1 shows the P-V and T-S diagrams (A, B) respectively. A diesel cycle consists of two isentropic processes where the entropy is constant, a process with constant pressure, and a constant

volume process. The 1–2 as well as 3–4 processes are isentropic processes, the 2–3 process is a constant pressure process, and the 4–1 is a constant volume process [74,75].

The heat input and output inside the diesel cycle can be calculated using Eqs 1 and 2 as following:

$$Q = m.C_p.(T_3 - T_2) \tag{1}$$

$$Q = m.C_v.(T_4 - T_1) \tag{2}$$

The thermal efficiency of the diesel cycle can be calculated by the Eq 3.

$$\eta = 1 - \frac{m.C_v.(T_4 - T_1)}{m.C_p.(T_3 - T_2)} = 1 - \frac{1}{\gamma}.\frac{(T_4 - T_1)}{(T_3 - T_2)} \tag{3}$$

The engine piston geometry is shown in Figure 2, which shows the top and bottom dead center pointes. Where the piston is moved within the different strokes of the engine cycle which are: the intake, the compression, the expansion, and the exhaust. In the illustration below the engine geometry can be studied.

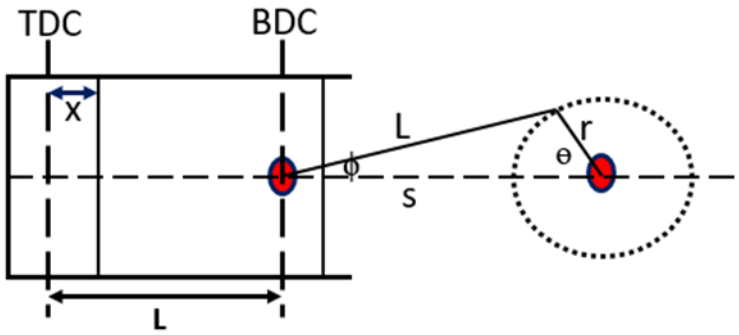

Figure 2. Geometry of the engine piston.

$$sin\emptyset = \frac{a}{L}.sin\theta \tag{4}$$

$$cos\emptyset = \sqrt{1 - sin^2\emptyset} \tag{5}$$

$$cos\emptyset = \sqrt{1 - \frac{a^2}{L^2}sin^2\theta} \tag{6}$$

The distance between the crank axis and the wrist pin axis (S) is given by:

$$s = a.cos\theta + \sqrt{L^2 - a^2.sin^2\theta} \tag{7}$$

Where the piston displacement from the TDC is given by:

$$s = a.cos\theta + \sqrt{L^2 - a^2.sin^2\theta} \tag{8}$$

Instantaneous piston speed is given by:

$$U_p = 2\pi N \left[a.sin\theta + \frac{a^2 sin\theta cos\theta}{\sqrt{L^2 - a^2 sin^2\theta}}\right] \quad (9)$$

Mean piston speed is given by:

$$\frac{U_p}{U_p} = \frac{\pi}{L} sin\theta \left[1 + \frac{cos\theta}{\sqrt{R^2 - sin^2\theta}}\right] \quad (10)$$

The power generated within the engine cylinder is referred to as indicated power. Whereas the real available power is called brake power. The difference between the indicated and breaking power is called the friction power. Overall, the mean effective engine pressure using the diesel cycle increases as the initial pressure increases.

3. Results and discussion

For the purposes of the present study, a four-stroke diesel engine was selected. The engine has 4 cylinders with an inline framework cooled by liquid water. The bore diameter is 160 mm, the piston travel is 190 mm, the engine reveal is 300 rpm, and the compression ratio is 25. The ambient conditions related to this study are 1 bar atmospheric pressure, and 288 K as a normal temperature. The purpose of the study was to study the impact of diesel fuel injection pressure on engine efficiency. Where the selected pressure is below 500, 500–800, 800–1000, and above 1000 bar for each test. At each injection pressure change, the engine performance parameter is examined and listed below.

The environment parameters of this study are fixed at the variable state of the injector pressure. As the static atmosphere pressure on the sea level is equal to 1 bar with a temperature of 288 K. The static ambient pressure and temperature are 1 bar and 288 K respectively. The exhaust backpressure is equal to 1 bar with the entire pressure of the injector selected. And the overall pressure after the induction air filter with a fixed value of 0.98 bar.

Figure 3 shows the parameters of the efficiency and power of the selected diesel engine in this study. There was a significant increase in piston engine power. As the injector pressure selected ranges from 91.8 kW at the injector pressure of less than 500 bar to 130.5 kW at the injector pressure of more than 1000 bar (See Figure 3A). The brake means effective pressure as well as the brake torque increase with the increase of the injector pressure (See Figure 3A).

The mass of fuel provided per cycle, specific fuel consumption, and specific fuel consumption in ISO are reduced. As the injector pressure increases where the values of the previous parameters are 0.127, 0.126, 0.126, and 0.126 g, 0.498, 0.376, 0.357, and 0.348 kg/kWh, and 0.50, 0.378, 0.358, and 0.349 kg/kWh respectively (See Figure 3B).

The efficiency of the piston engine, the indicated mean effective pressure, and the indicated efficiency increase significantly with the injector pressure increase as the maximum values of the specified parameters are 0.24, 6.8, and 0.48 respectively (See Figure 3C).

The friction means effective pressure as well as the mechanical efficiency of the piston engine are increased with the increasing of the injector pressure. The mean piston speed is remains constant with a value of 19 m/s with the increase in the injector pressure (See Figure 3D).

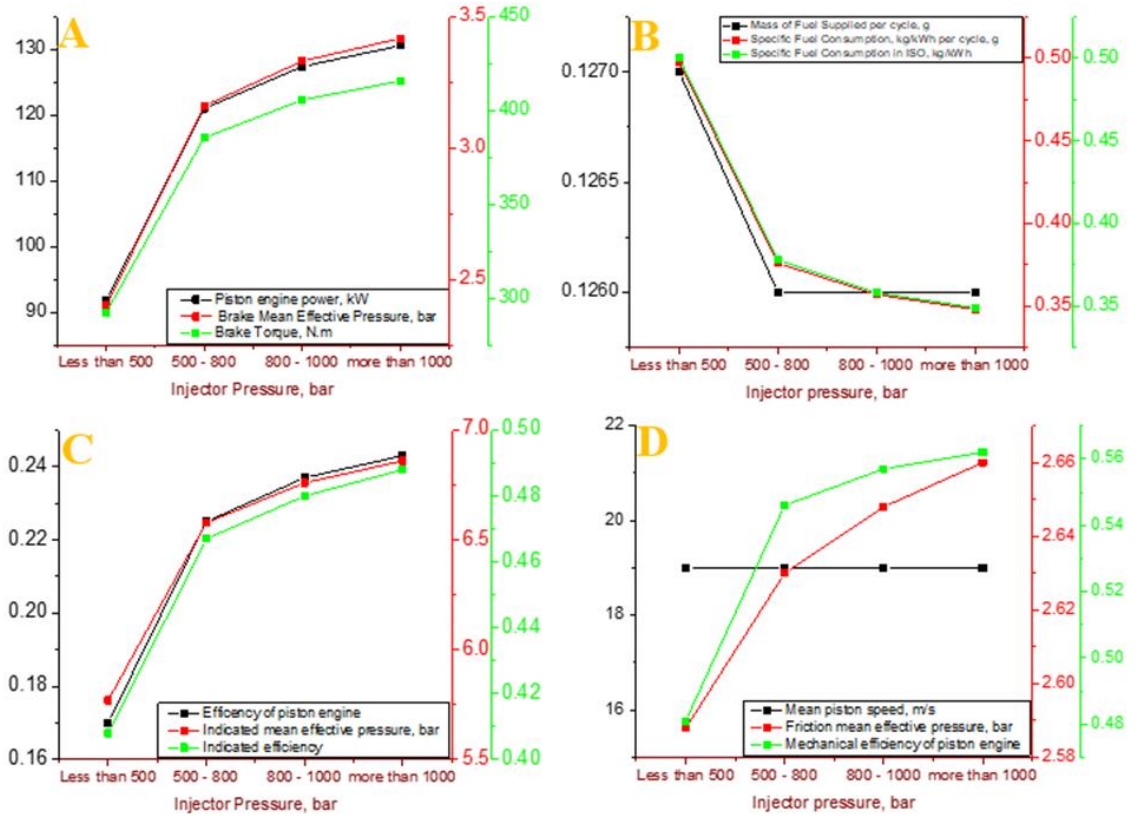

Figure 3. The parameters of efficiency and power. Piston engine power, and brake mean effective pressure, and the brake torque (A), the mass of fuel supplied per cycle, the specific fuel consumption, and the specific fuel consumption in ISO (B), the efficiency of the piston engine, the indicated mean effective pressure, and the indicated efficiency (C), and the mean piston speed, the friction means effective pressure, and the mechanical efficiency of the piston engine (D).

Table 1 presents the parameters of the selected engine inlet and exhaust system based on the variation in injector pressure. There was a slight increase in the mean inlet manifold temperature and the mean inlet manifold wall temperature with the increase in the injector pressure as the minimum value was 291.5, and 297.5 K at less than 500 bar injector pressure and 292, and 298 K at more than 1000 bar injector pressure respectively. A number of inlet system parameters decrease slightly as the injector pressure increases. For example, the average velocity of gases in the intake manifold, the heat transfer coefficient in the intake manifold, and the heat transfer coefficient in the intake port. The maximum speed in a central section of the inlet port and the total area of the effective valve port gorge remains constant during the injector pressure change. The average exhaust manifold gas temperature as well as the average exhaust manifold wall temperature decreased with the increase of the injector pressure. A small decree occurs at some exhaust parameters as the injector pressure increases. These include the Strouhal number, the maximum speed in the mid-section of the exhaust port, and the heat transfer coefficient in the exhaust manifold. The entire effective valve port throat area remains constant with the increase in injector pressure.

Table 1. Intake and exhaust parameters.

	Parameter	Symbol	Injector Pressure, bar Less than 500	500–800	800–1000	More than 1000
Intake system	Average intake manifold temperature, K	T_int	291.5	291.9	292.1	292
	Average gas velocity in intake manifold, m/s	v_int	48.45	48.3	48.2	48.2
	Average intake manifold wall temperature, K	Tw_int	297.5	297.9	298.1	298
	Heat transfer Coeff. in intake manifold, W/(m^2*K)	hc_int	71.1	70.8	70.6	70.5
	Heat transfer Coeff. in intake port, W/(m^2*K)	hc_int.p	301	300	299.8	299.3
	Max velocity in a middle section of Int. Port, m/s	v_int.p	95	95	95	95
	Total effective valve port throat area, cm^2	A_v.thrt	20.9	20.9	20.9	20.9
Exhaust System	Average exhaust manifold gas temperature, K	T_exh	909.2	851.9	823.8	805.5
	Average gas velocity in exhaust manifold, m/s	v_exh	79.4	75.2	72.9	71.7
	Strouhal number: Sh = a*Tau/L (has to be: Sh > 8)	Sh	10	9.7	9.58	9.4
	Average exhaust manifold wall temperature, K	Tw_exh	827.2	773.9	749.5	733.6
	Heat transfer Coeff. in exhaust manifold, W/(m^2*K)	hc_exh	215.5	210.2	207.9	206.7
	Heat transfer Coeff. in exhaust port, W/(m^2*K)	hc_exh.p	955.9	932.5	922.7	917.2
	Max velocity in a middle section of Exh. Port, m/s	v_exh.p	145	140	137	134.9
	Total effective valve port throat area, cm^2	A_v.thrt	19.9	19.9	19.9	19.9

The average inlet manifold pressure and the average exhaust manifold pressure remain constant at 0.96 and 1.04 bar as the injector pressure increases respectively. This provides an indication of the stability of the firing process inside the selected engine with the pressure variation of the injector.

Figure 4 shows the combustion parameters of the selected engine of the study with the variation of the injector pressure. The maximum cylinder temperature and pressure inside the engine increased from 1473.2 K, 81.2 bar at less than 500 bar injector pressure to 1805.2 K, 99 bar at more than 1000 bar respectively. Therefore, the engine combustion is enhanced by increasing the injector pressure (See Figure 4A). The maximum cylinder pressure angle remains constant at a value of 2 degrees as the pressure of the injector increases. During this time, the maximum temperature angle decreased as the injector pressure increased. Values were 26, 21, 18, and 17 degrees respectively with the chosen injector pressure values shown in Figure 4A. The maximum pressure rate rises sharply with the increase of the injector pressure (See Figure 4A). The maximum gas force acting on the engine piston and the maximum suction pressure increased with the increase in the injector pressure (See figure 4B).

The result indicates that engine performance is enhanced by increased injector pressure. Because the combustion temperature has increased in value each time.

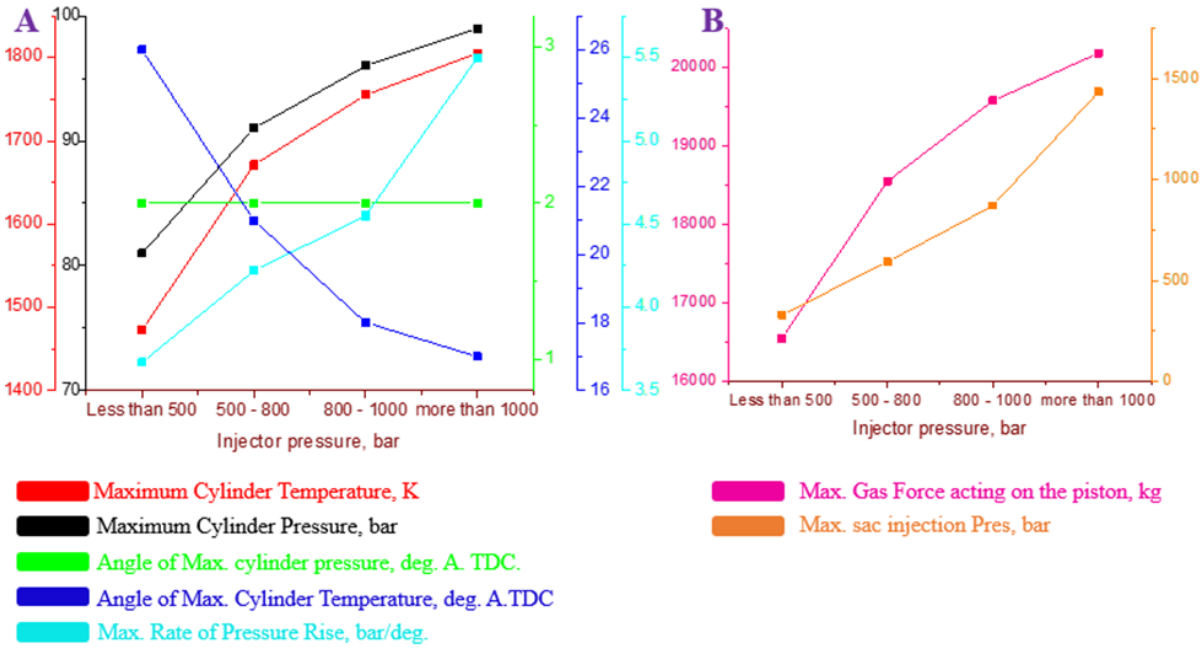

Figure 4. Max cylinder temperature, pressure, angle of Max. cylinder pressure, temperature, and Max rate of pressure rising (A), and Max. gas force acting on the piston, and suction injection pressure (B).

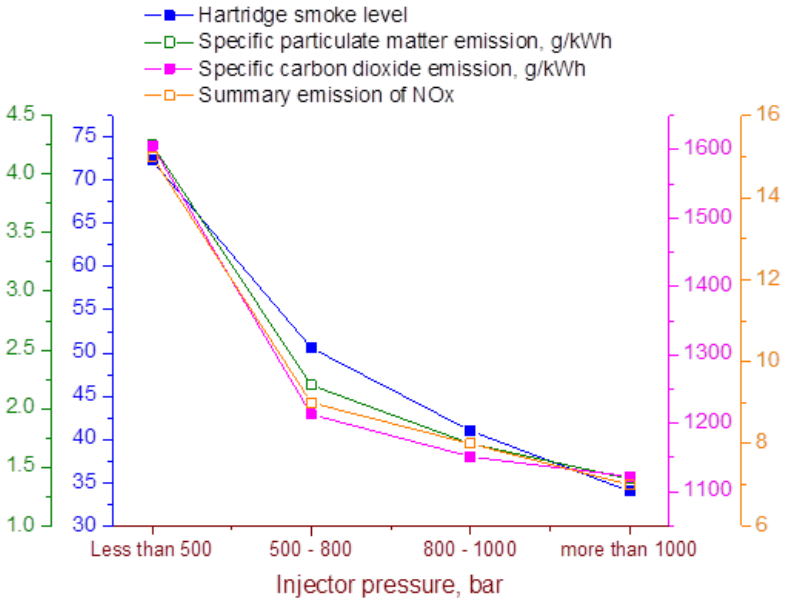

Figure 5. The ecological parameters of the selected engine.

Figure 5 shows the ecological parameters of the engine chosen for the study with the injection pressure variation. The engine smoke level, the specific particulate emissions, the specific carbon dioxide emissions, and the synthetic NOx emissions decrease considerably with the increase in injector pressure. The maximum reported parameter values are 72.3, 4.25, 1605.6, and 15 at the injector minimum pressure (i.e., less than 500 bar) respectively. Minimum values are 34, 1.4, 1122, and 7 at maximum injector pressure (i.e., higher than 1000 bar).

Table 2 shows the heat exchange parameter of the selected engine of the study with the variation of the injector pressure. The average equivalent temperature of the cycle, the average factor of heat transfers in the cylinder, and the average piston crown temperature are sharply increasing with the increase of the injector pressure as the average equivalent temperature of the cycle started to increase with the following values: 1020.4, 1088.4, 1118, and 1136.6 K respectively. The average factor of the heat transfers in the cylinder started to increase with the following values 449.7, 474.6, 485.68, and 495.09 W/m^2. K respectively. The average piston crown temperature started to increase with the following values 524.47, 543.74, 552.21, and 558.46 K respectively. The average cylinder liner temperature, and the boiling temperature in the liquid cooling system remain constant with the variation of the injector pressure at a value of 405, and 398 respectively. The rest of the heat exchange parameters are the average head wall temperature, the average temperature of cooled surface head of cylinder head, the average factor of heat transfers from head cooled surface to coolant, the heat flow in a cylinder head, the heat flow in a piston crown, and the heat flow in a cylinder liner are sharply increased with the increase of the injector pressure. The heat exchange parameters show an enhancement in the performance of the selected engine which reflects a result that indicates an increase of the injector pressure will enhance the engine performance with the same amount of the supplied fuel. This will result in more energy being used from the fuel energy supplied to the engine and less engine losses.

Table 2. Heat exchange parameters.

Parameter	Symbol	Injector pressure, bar			
		Less than 500	500–800	800–1000	More than 1000
Average equivalent temperature of cycle, K	T_eq	1020.4	1088.4	1118	1136.6
Aver. factor of heat transfer in Cyl., W/m^2, K	hc_c	449.7	474.6	485.7	495.1
Average piston crown temperature, K	Tw_pist	524.4	543.7	552.2	558.5
Average cylinder liner temperature, K	Tw_liner	405	405	405	405
Average head wall temperature, K	Tw_head	477	494.3	502	507.7
Average temperature of cooled surface head of cylinder head, K	Tw_cool	378.2	379.9	381.2	381.8
Boiling Temp. in liquid cooling system, K	Tboil	398	398	398	398
Average factor of heat transfer, W/(m2*K) from head cooled surface to coolant	hc_cool	9826.1	10337	10670	10841
Heat flow in a cylinder head, J/s	q_head	4915.5	5668.6	6014.7	6260.7
Heat flow in a piston crown, J/s	q_pist	4484.2	5196.9	5524.7	5755.1
Heat flow in a cylinder liner, J/s	q_liner	5704.9	5408.2	5195.6	5035

4. Conclusions

This study highlights the effect of the injection pressure increase on the engine to complete the ignition cycle and examines the impact of this increase on engine performance. All performance parameters were observed to be affected by the increase in injector pressure. Consequently, the engine's performance improved.

The compression stroke temperature was increased sharply with the increase of the injector pressure as the temperature for the four trials was 1092, 1097, 1099, and 1101 K for the injector pressure of less than 500, 500–800, 800–1000, and more than 1000 respectively. Temperature rise is an indicator of the performance improvement of the engine selected in this study.

The increase of the injector pressure aids in enhancement on the emission that comes out of the engine during the operation as the amount of the carbon dioxide, SOx, and NOx are sharply decreased by increasing the injector pressure. It is noted that the increase in the injector pressure enhanced the heat exchange inside the engine as the coefficients of the heat transfer inside the engine affected positively by that increment in the injector pressure.

The exhaust parameter reflects an improvement in engine performance as all exhaust parameters demonstrate a positive impact on engine performance. As a result of that, the average exhaust manifold gas temperature sharply decreased from 909 to 805 K in this study, which is an indicator of the enhancement that occurred to the engine.

Such investigation will aid in improving the performance of the internal combustion engines by highlighting the points where the development can perform and expand to affect the design of the engine to face the new needs.

Conflict of interest

The author declares no conflict of interests for this article.

References

1. Pham Q, Park S, Agarwal AK, et al. (2022) Review of dual-fuel combustion in the compression-ignition engine: Spray, combustion, and emission. *Energy* 250: 123778. https://doi.org/10.1016/j.energy.2022.123778
2. Chen L, Xu ZP, Liu SS, et al. (2022) Dynamic modeling of a free-piston engine based on combustion parameters prediction. *Energy* 249: 123792. https://doi.org/10.1016/j.energy.2022.123792
3. Sinigaglia T, Martins MES, Cezar Mairesse Siluk J (2022) Technological evolution of internal combustion engine vehicle: A patent data analysis. *Appl Energy* 306: 118003. https://doi.org/10.1016/j.apenergy.2021.118003
4. Wang Z, Su X, Wang X, et al. (2022) Impact of ignition energy on the combustion performance of an SI heavy-duty stoichiometric operation natural gas engine. *Fuel* 313: 122857. https://doi.org/10.1016/j.fuel.2021.122857
5. Aliramezani M, Koch CR, Shahbakhti M (2022) Modeling, diagnostics, optimization, and control of internal combustion engines via modern machine learning techniques: A review and future directions. *Prog Energy Combust Sci* 88: 100967. https://doi.org/10.1016/j.pecs.2021.100967
6. Şanlı A, Yılmaz İT (2022) Cycle-to-cycle combustion analysis in hydrogen fumigated common-rail diesel engine. *Fuel* 320: 123887. https://doi.org/10.1016/j.fuel.2022.123887
7. Abu Qadourah J, Al-Falahat AM, Alrwashdeh SS, et al. (2022) Improving the energy performance of the typical multi-family buildings in Amman, Jordan. *City Territ Archit* 9. https://doi.org/10.1186/s40410-022-00151-8

8. Al-Falahat AM, Kardjilov N, Khanh TV, et al. (2019) Energy-selective neutron imaging by exploiting wavelength gradients of double crystal monochromators—Simulations and experiments. *Nucl Instrum Methods Phys Res A: Accel Spectrom Detect Assoc Equip* 943: 162477. https://doi.org/10.1016/j.nima.2019.162477
9. Al-Falahat AM, Qadourah JA, Alrwashdeh SS (2022) Economic feasibility of heating source conversion of the swimming pools. *J Appl Eng Sci* 20: 230–238. https://doi.org/10.5937/jaes0-34474
10. Al-Falahat AM, Qadourah JA, Alrwashdeh SS, et al. (2022) Energy performance and economics assessments of a photovoltaic-heat pump system. *Results Eng* 13: 100324. https://doi.org/10.1016/j.rineng.2021.100324
11. Alrwashdeh SS (2017) Determining the optimum tilt solar angle of a PV applications at different sites in Jordan. *J Eng Appl Sci* 12: 9295–9303. Available from: http://jjmie.hu.edu.jo/vol9-3/JJMIE-181-14-01%20Proof%20Reading%20ok.pdf.
12. Shi C, Zhang P, Ji C, et al. (2022) Understanding the role of turbulence-induced blade configuration in improving combustion process for hydrogen-enriched rotary engine. *Fuel* 319: 123807. https://doi.org/10.1016/j.fuel.2022.123807
13. Park J, Oh J (2022) Study on the characteristics of performance, combustion, and emissions for a diesel water emulsion fuel on a combustion visualization engine and a commercial diesel engine. *Fuel* 311: 122520. https://doi.org/10.1016/j.fuel.2021.122520
14. Gonca G (2016) Comparative performance analyses of irreversible OMCE (Otto Miller cycle engine)-DiMCE (Diesel miller cycle engine)-DMCE (Dual Miller cycle engine). *Energy* 109: 152–159. https://doi.org/10.1016/j.energy.2016.04.049
15. Gamiño B, Aguillón J (2010) Numerical simulation of syngas combustion with a multi-spark ignition system in a diesel engine adapted to work at the Otto cycle. *Fuel* 89: 581–591. https://doi.org/10.1016/j.fuel.2009.06.030
16. Guo Q, Liu J, Wu BY, et al. (2022) On the optimization of the double-layer combustion chamber with and without EGR of a diesel engine. *Energy* 247: 123486. https://doi.org/10.1016/j.energy.2022.123486
17. Alrwashdeh SS (2018) Predicting of energy production of solar tower based on the study of the cosine efficiency and the field layout of heliostats. *Int J Mech Eng Technol* 9: 250–257. Available from: https://iaeme.com/MasterAdmin/Journal_uploads/IJMET/VOLUME_9_ISSUE_11/IJMET_09_11_026.pdf.
18. Alrwashdeh SS (2018) Investigation of the energy output from PV racks based on using different tracking systems in Amman-Jordan. *Int J Mech Eng Technol* 9: 687–694. Available from: https://iaeme.com/MasterAdmin/Journal_uploads/IJMET/VOLUME_9_ISSUE_10/IJMET_09_10_071.pdf.
19. Alrwashdeh SS (2018) Comparison among solar panel arrays production with a different operating temperatures in Amman-Jordan. *Int J Mech Eng Technol* 9: 420–429. Available from: https://iaeme.com/MasterAdmin/Journal_uploads/IJMET/VOLUME_9_ISSUE_6/IJMET_09_06_047.pdf.

20. Alrwashdeh SS (2018) Energy production evaluation from a linear fresnel reflectors arrays with different array orientation. *Int J Eng Res* 11: 1811–1819. Available from: https://www.ripublication.com/irph/ijert18/ijertv11n11_11.pdf.
21. Alrwashdeh SS (2018) Assessment of the energy production from PV racks based on using different solar canopy form factors in Amman-Jordan. *Int J Eng Res* 11: 1595–1603. Available from: https://www.ripublication.com/irph/ijert18/ijertv11n10_09.pdf.
22. He D, Yu Y, Wang C, et al. (2022) Maximum specific cycle net-work based performance analyses and optimizations of thermodynamic gas power cycles. *Case Stud Therm Eng* 32: 101865. https://doi.org/10.1016/j.csite.2022.101865
23. Alrwashdeh SS (2018) The effect of solar tower height on its energy output at Ma'an-Jordan. *AIMS Energy* 6: 959–966. https://doi.org/10.3934/energy.2018.6.959
24. Alrwashdeh SS (2018) Modelling of operating conditions of conduction heat transfer mode using energy 2D simulation. *Int J Online Eng* 14: 200–207. https://doi.org/10.3991/ijoe.v14i09.9116
25. Alrwashdeh SS (2018) Assessment of photovoltaic energy production at different locations in Jordan. *Int J Renewable Energy Res* 8: 797–804. Available from: http://www.ijrer.com/index.php/ijrer/article/view/7337.
26. Alrwashdeh SS (2019) An energy production evaluation from PV arrays with different inter-row distances. *Int J Mech Prod Eng Res Dev* 9: 1–10. Available from: http://www.tjprc.org/publishpapers/2-67-1565948586-1IJMPERDOCT20191.pdf.
27. Alrwashdeh SS (2019) Energy production assessment of solar tower based on the study of the mirror shadowing and blocking effects. *Univers J Mech Eng* 7: 71–76. https://doi.org/10.13189/ujme.2019.070205
28. Jafari H, Yang W, Ryu C (2020) Evaluation of a distributed combustion concept using 1-D modeling for pressurized oxy-combustion system with low flue gas recirculation. *Fuel* 263: 116723. https://doi.org/10.1016/j.fuel.2019.116723
29. Negoro AB, Purwadi A (2013) Performance analysis on power train drive system of the 2012 toyota camry hybrid. *Procedia Technol* 11: 1054–1064. https://doi.org/10.1016/j.protcy.2013.12.294
30. Doppalapudi AT, Azad AK, Khan MMK (2021) Combustion chamber modifications to improve diesel engine performance and reduce emissions: A review. *Renewable Sustainable Energy Rev* 152: 111683. https://doi.org/10.1016/j.rser.2021.111683
31. Zarenezhad Ashkezari A (2022) Numerical analysis of performance and emissions behavior of a bi-fuel engine with compressed natural gas enriched with hydrogen using variable compression ratio strategy. *Int J Hydrogen Energy* 47: 10762–10776. https://doi.org/10.1016/j.ijhydene.2022.01.129
32. Agarwal AK, Kumar V, Ankur Kalwar AJ (2022) Fuel injection strategy optimisation and experimental performance and emissions evaluation of diesel displacement by port fuel injected methanol in a retrofitted mid-size genset engine prototype. *Energy* 248: 123593. https://doi.org/10.1016/j.energy.2022.123593
33. Liu JH, Wu PC, Ji Q, et al. (2022) Experimental study on effects of pilot injection strategy on combustion and emission characteristics of diesel/methanol dual-fuel engine under low load. *Energy* 247: 123464. https://doi.org/10.1016/j.energy.2022.123464

34. Alrwashdeh SS (2019) Investigation of wind energy production at different sites in Jordan using the site effectiveness method. *J Energy Eng* 116: 47–59. https://doi.org/10.1080/01998595.2019.12043338
35. Alrwashdeh SS (2021) Investigation of the energy output from PV panels based on using different orientation systems in Amman-Jordan. *Case Stud Therm Eng* 28: 101580. https://doi.org/10.1016/j.csite.2021.101580
36. Alrwashdeh SS (2022) Energy sources assessment in Jordan. *Results Eng* 13: 100329. https://doi.org/10.1016/j.rineng.2021.100329
37. Alrwashdeh SS, Alsaraireh FM (2018) Wind energy production assessment at different sites in Jordan using probability distribution functions. *ARPN J Eng Appl Sci* 13: 8163–8172. Available from: http://www.arpnjournals.org/jeas/research_papers/rp_2018/jeas_1018_7317.pdf.
38. Alrwashdeh SS, Alsaraireh FM, Saraireh MA, et al. (2018) In-situ investigation of water distribution in polymer electrolyte membrane fuel cells using high-resolution neutron tomography with 6.5 μm pixel size. *AIMS Energy* 6: 607–614. https://doi.org/10.3934/energy.2018.4.607
39. Kale AV, Krishnasamy A (2022) Effects of variations in fuel properties on a homogeneous charge compression ignited light-duty diesel engine operated with gasoline-isobutanol blends. *Energy Convers Manage* 258: 115373. https://doi.org/10.1016/j.enconman.2022.115373
40. Paykani A, Chehrmonavari H, Tsolakis A, et al. (2022) Synthesis gas as a fuel for internal combustion engines in transportation. *Prog Energy Combust Sci* 90: 100995. https://doi.org/10.1016/j.pecs.2022.100995
41. Olanrewaju FO, Li H, Aslam Z, et al. (2022) Analysis of the effect of syngas substitution of diesel on the Heat Release Rate and combustion behaviour of Diesel-Syngas dual fuel engine. *Fuel* 312: 122842. https://doi.org/10.1016/j.fuel.2021.122842
42. Figari M, Theotokatos G, Coraddu A, et al. (2022) Parametric investigation and optimal selection of the hybrid turbocharger system for a large marine four-stroke dual-fuel engine. *Appl Therm Eng* 208: 117991. https://doi.org/10.1016/j.applthermaleng.2021.117991
43. Kumar Sethi C, Parimita Patnaik P, Kumar Acharya S, et al. (2022) An efficient approach for emission reduction in diesel engine with ferric chloride as catalyst and yttria stabilized zirconia as thermal barrier coating. *Mater Today: Proc.* https://doi.org/10.1016/j.matpr.2022.03.317
44. Teoh YH, Yaqoob H, How HG, et al. (2022) Comparative assessment of performance, emissions and combustion characteristics of tire pyrolysis oil-diesel and biodiesel-diesel blends in a common-rail direct injection engine. *Fuel* 313: 123058. https://doi.org/10.1016/j.fuel.2021.123058
45. Huang Z, Huang J, Luo J, et al. (2022) Performance enhancement and emission reduction of a diesel engine fueled with different biodiesel-diesel blending fuel based on the multi-parameter optimization theory. *Fuel* 314: 122753. https://doi.org/10.1016/j.fuel.2021.122753
46. Sharma H, Mahla SK, Dhir A (2022) Effect of utilization of hydrogen-rich reformed biogas on the performance and emission characteristics of common rail diesel engine. *Int J Hydrogen Energy* 47: 10409–10419. https://doi.org/10.1016/j.ijhydene.2022.01.073
47. Veza I, Karaoglan AD, Ileri E, et al. (2022) Grasshopper optimization algorithm for diesel engine fuelled with ethanol-biodiesel-diesel blends. *Case Stud Therm Eng* 31: 101817. https://doi.org/10.1016/j.csite.2022.101817

48. Alrwashdeh SS, Ammari H (2019) Life cycle cost analysis of two different refrigeration systems powered by solar energy. *Case Stud Therm Eng* 16: 100559. https://doi.org/10.1016/j.csite.2019.100559
49. Alrwashdeh SS, Ammari H, Madanat MA, et al. (2022) The effect of heat exchanger design on heat transfer rate and temperature distribution. *Emerg Sci J* 6: 128–137. https://doi.org/10.28991/ESJ-2022-06-01-010
50. Alrwashdeh SS, Manke I, Markötter H, et al. (2017) Improved performance of polymer electrolyte membrane fuel cells with modified microporous layer structures. *Energy Technol* 5: 1612–1618. https://doi.org/10.1002/ente.201700005
51. Alrwashdeh SS, Manke I, Markötter H, et al. (2017) Neutron radiographic in operando investigation of water transport in polymer electrolyte membrane fuel cells with channel barriers. *Energy Convers Manage* 148: 604–610. https://doi.org/10.1016/j.enconman.2017.06.032
52. Alrwashdeh SS, Manke I, Markötter H, et al. (2017) In operando quantification of three-dimensional water distribution in nanoporous carbon-based layers in polymer electrolyte membrane fuel cells. *ACS Nano* 11: 5944–5949. https://doi.org/10.1021/acsnano.7b01720
53. Li R, Wen C, Meng X, et al. (2022) Measurement of the friction force of sliding friction pairs in low-speed marine diesel engines and comparison with numerical simulation. *Appl Ocean Res* 121: 103089. https://doi.org/10.1016/j.apor.2022.103089
54. Chen HY, Cheng Y, He QG, et al. (2022) Experimental study on combustion and unregulated emission characteristics of a diesel engine fueled with light hydrocarbon/diesel blends. *Fuel* 315: 123075. https://doi.org/10.1016/j.fuel.2021.123075
55. Alrwashdeh SS, Markötter H, Haußmann J, et al. (2016) Investigation of water transport dynamics in polymer electrolyte membrane fuel cells based on high porous micro porous layers. *Energy* 102: 161–165. https://doi.org/10.1016/j.energy.2016.02.075
56. Alrwashdeh SS, Markötter H, Haußmann J, et al. (2016) X-ray tomographic investigation of water distribution in polymer electrolyte membrane fuel cells with different gas diffusion media. *ECS Trans* 72. https://doi.org/10.1149/07208.0099ecst
57. Altarawneh OR, Alsarayreh AA, Al-Falahat AM, et al. (2022) Energy and exergy analyses for a combined cycle power plant in Jordan. *Case Stud Therm Eng* 31: 101852. https://doi.org/10.1016/j.csite.2022.101852
58. Ammari HD, Al-Rwashdeh SS, Al-Najideen MI (2015) Evaluation of wind energy potential and electricity generation at five locations in Jordan. *Sustain Cities Soc* 15: 135–143. https://doi.org/10.1016/j.scs.2014.11.005
59. Göbel M, Kirsch S, Schwarze L, et al. (2018) Transient limiting current measurements for characterization of gas diffusion layers. *J Power Sources* 402: 237–245. https://doi.org/10.1016/j.jpowsour.2018.09.003
60. Ince UU, Markötter H, George MG, et al. (2018) Effects of compression on water distribution in gas diffusion layer materials of PEMFC in a point injection device by means of synchrotron X-ray imaging. *Int J Hydrogen Energy* 43: 391–406. https://doi.org/10.1016/j.ijhydene.2017.11.047
61. Zhang Z, Tian J, Xie G, et al. (2022) Investigation on the combustion and emission characteristics of diesel engine fueled with diesel/methanol/n-butanol blends. *Fuel* 314: 123088. https://doi.org/10.1016/j.fuel.2021.123088

62. Demir U, Kozan A, Özer S (2022) Experimental investigation of the effect of urea addition to fuel on engine performance and emissions in diesel engines. *Fuel* 311: 122578. https://doi.org/10.1016/j.fuel.2021.122578
63. Kodate SV, Raju PS, Yadav AK, et al. (2022) Effect of fuel preheating on performance, emission and combustion characteristics of a diesel engine fuelled with Vateria indica methyl ester blends at various loads. *J Environ Manage* 304: 114284. https://doi.org/10.1016/j.jenvman.2021.114284
64. Can Ö, Baklacioglu T, Özturk E, et al (2022) Artificial neural networks modeling of combustion parameters for a diesel engine fueled with biodiesel fuel. *Energy* 247: 123473. https://doi.org/10.1016/j.energy.2022.123473
65. Markötter H, Manke I, Böll J, et al. (2019) Morphology correction technique for tomographic in-situ and operando studies in energy research. *J Power Sources* 414: 8–12. https://doi.org/10.1016/j.jpowsour.2018.12.072
66. Saraireh MA, Alsaraireh FM, Alrwashdeh SS (2017) Investigation of heat transfer for staggered and in-line tubes. *Int J Mech Eng Technol* 8: 476–483. Available from: https://iaeme.com/MasterAdmin/Journal_uploads/IJMET/VOLUME_8_ISSUE_11/IJMET_08_11_051.pdf.
67. Sun F, Markötter H, Manke I, et al. (2017) Complementary X-ray and neutron radiography study of the initial lithiation process in lithium-ion batteries containing silicon electrodes. *Appl Surf Sci* 399: 359–366. https://doi.org/10.1016/j.apsusc.2016.12.093
68. Sun F, Markötter H, Zhou D, et al. (2016) In situ radiographic investigation of (De)Lithiation mechanisms in a tin-electrode lithium-ion battery. *Chem Sus Chem* 9: 946–950. https://doi.org/10.1002/cssc.201600220
69. Ma B, Yao A, Yao C, et al. (2021) Multiple combustion modes existing in the engine operating in diesel methanol dual fuel. *Energy* 234: 121285. https://doi.org/10.1016/j.energy.2021.121285
70. Kalil Rahiman M, Santhoshkumar S, Subramaniam D, et al. (2022) Effects of oxygenated fuel pertaining to fuel analysis on diesel engine combustion and emission characteristics. *Energy* 239: 122373. https://doi.org/10.1016/j.energy.2021.122373
71. Zhao Z, Cui H (2022) Numerical investigation on combustion processes of an aircraft piston engine fueled with aviation kerosene and gasoline. *Energy* 239: 122264. https://doi.org/10.1016/j.energy.2021.122264
72. Öztürk E, Can Ö (2022) Effects of EGR, injection retardation and ethanol addition on combustion, performance and emissions of a DI diesel engine fueled with canola biodiesel/diesel fuel blend. *Energy* 244: 123129. https://doi.org/10.1016/j.energy.2022.123129
73. Sahu MK, Singh AK, Choudhary T (2022) Experimental investigation of thermal potential at diesel engine exhaust and numerical simulation of heat recovery in heat exchangers. *Mater Today: Proc* 56: 220–225. https://doi.org/10.1016/j.matpr.2022.01.076
74. Tipanluisa L, Thakkar K, Fonseca N, et al. (2022) Investigation of diesel/n-butanol blends as drop-in fuel for heavy-duty diesel engines: Combustion, performance, and emissions. *Energy Convers Manage* 255: 115334. https://doi.org/10.1016/j.enconman.2022.115334

75. Rakopoulos CD, Rakopoulos DC, Kyritsis DC, et al. (2022) Exergy evaluation of equivalence ratio, compression ratio and residual gas effects in variable compression ratio spark-ignition engine using quasi-dimensional combustion modeling. *Energy* 244: 123080. https://doi.org/10.1016/j.energy.2021.123080

AIMS Press